Research Article ISSN 2689-1050

Chemical & Pharmaceutical Research

Identification and anti-viral activities of butanolide skeleton from Cinnamomum kotoense and Cinnamomum subavenium by inhibiting H5N1 neuraminidase

Chang C.T.[1], Liu C.M.[2], Yeh H.C.[3], Li W.J.[4], Li H.T.[5], Chen C.Y.[3*] and Liu S.L.[6*]

[1]*Department of Clinical Microbiology Laboratory, Yuan's General Hospital, Kaohsiung, Taiwan.*

[2]*School of Medicine, Yichun University, 576 XueFu Road, Yuanzhou District, Yichun 336000, China*

[3]*School of Medical and Health Sciences, Fooyin University, Kaohsiung 83102, Taiwan.*

[4]*School of Nursing, Fooyin University, Kaohsiung 83102, Taiwan.*

[5]*Department of Medical Laboratory Science and Biotechnology, Fooyin University, Kaohsiung 83102, Taiwan.*

[6]*Experimental Forest, College of Bio-Resources and Agriculture, National Taiwan University, Nantou County, Taiwan.*

***Correspondence:**

Chen C.Y., School of Medical and Health Sciences, Fooyin University, Kaohsiung 83102, Taiwan.

Liu S.L., Experimental Forest, College of Bio-Resources and Agriculture, National Taiwan University, Nantou County, Taiwan.

Received: 02 Apr 2022; **Accepted:** 30 Apr 2022; **Published:** 05 May 2022

Citation: Chang CT, Liu CM, Yeh HC, et al. Identification and anti-viral activities of butanolide skeleton from Cinnamomum kotoense and Cinnamomum subavenium by inhibiting H5N1 neuraminidase . Chem Pharm Res. 2022; 4(2): 1-7.

ABSTRACT

The human influenza virus and avian influenza virus represents a serious threat to human health. Although zanamivir and oseltamivir against influenza virus neuraminidase and thus the viral replication is not available. The oseltamivir-resistant H5N1 virus has been isolated from patient. Moreover, several cases have been reported where patients developed adverse symptoms due to a long-term use of oseltamivir. Effective antiviral drugs are essential for early control of an influenza pandemic. Natural products have been used as important resources for medicine and healthy food to improve the quality of life. Cinnamon bark is widely used as a spice and herb medicine. In this study, we have isolated and identified three butanolide derivatives, kotomolide A, isolinderanolide B and linderanolide B from Cinnamomum kotoense and Cinnamomum subavenium. Further, enzyme-based screening and anti-viral activity were also examined. Our study provides a starting point for developing new therapeutic or preventive agents from natural products for avian influenza virus.

Keywords

Cinnamomum kotoense, Cinnamomum subavenium, Neuraminidase.

Introduction

Influenza or flu is affecting both humans and animals usually in winter or early spring every year. This disease is caused by the filterable virus, a sub-group of the Orthomyxoviridae. The viruses are divided into types A, B and C based on the serum immune response reactions of antigenic differences, and significant medical problems in humans are usually caused by type A. The virus usually invades the lung via the mouth and nose and causes fever and respiratory problems. Every 3 to 4 years there is an outbreak, and a major epidemic occurs worldwide once every 10 to 30 years [1]. Children are most vulnerable due to relative immunodeficiency and are largely responsible for transmission of influenza viruses in the community. The elderly and persons with underlying health problems are at increased risk for complications and hospitalization from influenza infection.

The influenza virus is a human respiratory pathogen especially influenza A. Influenza A can lead to significant morbidity and mortality each year. Influenza A is divided into various subtypes, depending on their envelope glycoproteins. There have been three major influenza virus pandemics in the last century. The 1957 (H_2N_2) and 1968 (H_3N_2) pandemic viruses were avian-human reassortments in which three and two of the eight avian gene segments, respectively, were reassorted into an already circulating, human-adapted virus [2,3]. The extinct pandemic virus from 1918 which killed 50 million people worldwide [4] have been reconstructed in the laboratory and was found to be highly virulent in mice and chicken embryos [5,6]. The H5N1 avian influenza virus, commonly called bird flu, is a highly contagious and deadly pathogen in poultry. Since late 2003, H5N1 has reached epizootic levels in domestic fowls in Asian countries and spread to much of Europe and into Africa via infected wild bird populations. By mutations in HA to change the receptor specificity, the bird flu virus has gained the ability to infect humans. As of 4 April 2006, there have been 191 severe infections with a high mortality of 108 deaths in Indonesia, Vietnam, Thailand, Cambodia, China, Iraq, Turkey, Azerbaijan, and Egypt.

Currently anti-influenza A drugs are mainly directed against the viral M2 protein and neuraminidase. NA has been served as a drug target to identify Zanamivir and Oseltamivir. However, the oseltamivir-resistant H5N1 virus has been isolated from a Vietnamese patient [7]. It is urgent to develop new drugs for treatment or prevention of the disease. Some natural plant products are known as important medicinal resources because they contain active substances that cause certain reactions on the human organism

In this study, we have identified novel inhibitors of NA from Cinnamomum kotoense and Cinnamomum subavenium. Cinnamomum kotoense (Lauraceae), which is a small evergreen tree, endemic to Lanyu Island of Taiwan, and has recently been cultivated as an ornamental plant [8] as well as Cinnamomum subavenium Miq. (Lauraceae), which is a medium-sized evergreen tree, found in central to southern mainland China, Burma, Cambodia, Taiwan, Malaysia, and Indonesia [8]. There are a few papers describing the constituents of Cinnamomum kotoense [9-11]. As described in this study, we isolated the phytochemicals and examined the anti-virus activity by using enzyme-based screening system. We discovered the lead compounds which effectively inhibited the neuraminidase of H5N1 avian influenza virus from these plants.

Materials and Methods

Expression and Purification of H5N1 NA

Full-length cDNA encoding the same amino acid sequence corresponding to the neuraminidase (NA) from A/Hanoi/30408/2005(H5N1) influenza virus was synthesized by Geneart Company (BioPark, Germany). The cDNA encoding N-terminal His-tagged ectodomain (63-449) of NA protein was engineered using sticky-end polymerase chain reaction (PCR) with EcoRI/PstI restriction site and cloned into the baculovirus transfer vector, pAcGP67-A (BD Biosciences Pharmingen, San Jose, CA). The primers used in the sticky-end PCR were designed as follows: forward primers 1 (5'-AATTCCACCATCACCATCACCATGTGAAGCTGGCTGGTAACTCCTCC) and 2 (5'-CCACCATCACCATCACCATGTGAAGCTGGCTGGTAACTCCTCC); reverse primers 1 (5'-TCGAGTTACTTGTCGATGGTGAAGGGCAGCTC) and 2 (5'-GTTACTTGTCGATGGTGAAGGGCAGCTC). The recombinant NA-pAcGP67-A vector was amplified in *E. coli* strain, JM109, under ampicillin selection. The co-transfection of the recombinant NA-pAcGP67-A vector and BaculoGold linearized baculovirus DNA (BD Biosciences Pharmingen) was carried out in insect Spodopterafrugiperda (Sf9) cells (Invitrogen, Carlsbad, CA).

Insect Sf9 cells (2 x 107/ml) were cultured in Sf-900 II medium (Invitrogen) supplemented with 5% fetal bovine serum (Sigma, St Louis, MO). After the cells had attached, the medium was removed, and the cells were infected with the recombinant baculovirus virus at a multiplicity of infection (MOI) of 10 for 3 days at 27°C. Culture media were collected, concentrated using 100K-limited Amicon Ultra-15 centrifugal filter device (Milliproe, Cork, Ireland), and dialyzed against buffer A on day 3 [20 mM Tris-HCl (pH 7.5), 150 mM NaCl, 10 mM imidazole] containing 5 mM $MgCl_2$ and $CaCl_2$. Subsequently, the dialyzed media were subjected to metal affinity chromatography using Ni-NTA resin (Amersham Bioscience, Tokyo, Japan). The Ni2+-bound proteins were washed with 10 volumes of buffer A [20 mM Tris-HCl (pH 7.5), 150 mM NaCl, 10 mM imidazole] and then eluted with buffer B [20 mM Tris-HCl (pH 7.5), 150 mM NaCl, 500 mM imidazole] in a linear gradient of 10 to 500 mM imidazole. The fractions containing NA tetramer were pooled and dialyzed against phosphate-buffered saline (PBS), pH 7.4, to remove imidazole.

Purification of active ingredients from the C. kotoense and C. subavenium

Pure components were isolated from the leaves of C. kotoense and stems of C. subavenium for screening their anti-NA activities. 100 μM of kotomolide A, isolinderanolide B and linderanolide B were examined for NA inhibition. Kotomolide A was isolated from the leaves of C. kotoense as described previously [10]. Briefly, the air-dried leaves were extracted with MeOH at room temperature, and the MeOH extract was obtained upon concentration under reduced pressure. The MeOH extract, suspended in H_2O, was partitioned with $CHCl_3$ to give fractions soluble in $CHCl_3$ and H_2O. The CHC_3 soluble fraction was subjected to chromatograph over silica gel using n-hexane-EtOAc-acetone as eluent to yield five fractions. Fraction II was re-subjected to silica gel CC and purified by preparative TLC using n-hexane-EtOAc to yield kotomolide A (Figure 1).

Isolinderanolide B and Linderanolide B were isolated from the stems of *C. subavenium* as described previously [12]. Briefly, the air-dried stems were extracted with MeOH at room temperature and the MeOH extract was obtained upon concentration under reduced pressure. The MeOH extract, suspended in H_2O, was partitioned with $CHCl_3$ to give fractions soluble in $CHCl_3$ and

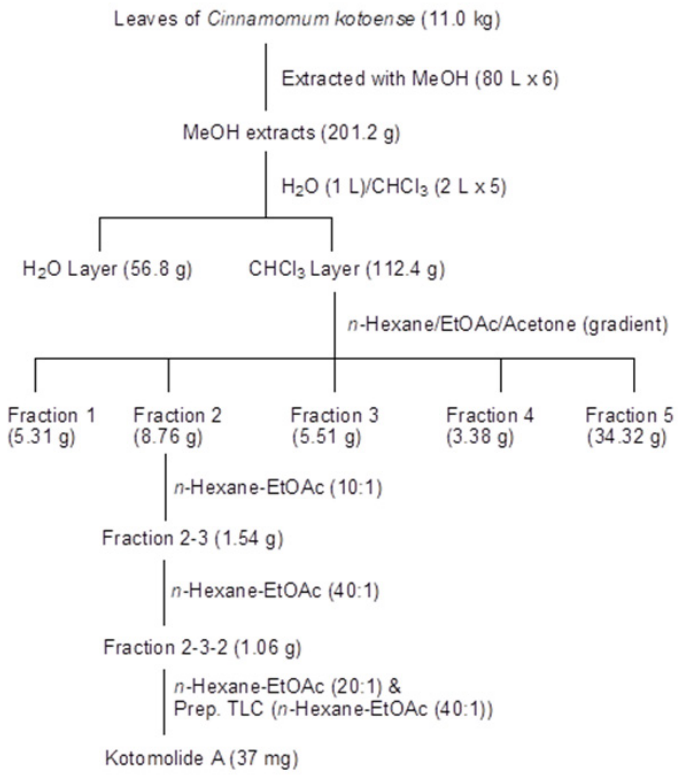

Figure 1: The extraction process of Kotomolide A from leaves from Cinnamomum kotoense.

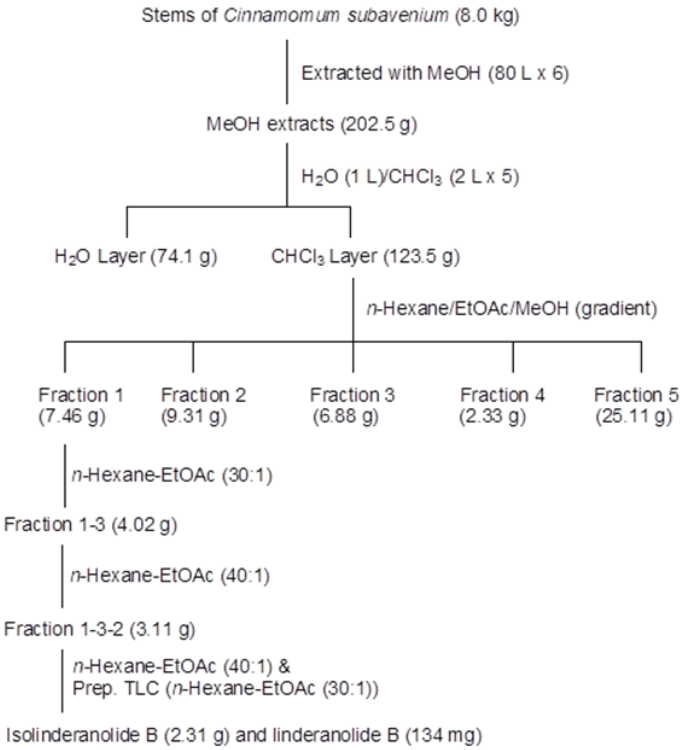

Figure 2: The extraction process of isolinderanolide B and iinderanolide B from stems from *Cinnamomum subavenium*.

H_2O. The CHC_3 soluble fraction was subjected to chromatograph over silica gel using n-hexane/EtOAc/MeOH mixtures as eluents to produce five fractions. Part of fraction 1 was subjected to silica gel chromatography by eluting with n-hexane-EtOAc (30:1), enriched with EtOAc to furnish ten fractions (1-1-1-10). Fraction 1-3 was subjected to silica gel chromatography, eluting with n-hexane-EtOAc (40:1) and enriched gradually with EtOAc, to obtain three fractions (1-3-1-1-3-3). Fraction 1-3-2 (3.11 g), eluted with n-hexane-EtOAc (40:1), was further separated using silica gel column chromatography and preparative TLC (n-hexane-EtOAc (30:1) and gave isolinderanolide B (2.31 g) and linderanolide B (134 mg) (Figure 2).

Kinetic and inhibition assays of recombinant NA

The enzyme kinetic assay was performed by monitoring the NA activity of recombinant H5N1 neuraminidase in the presence of serial diluted fluorogenic NA substrate 2'-(4-methylumbelliferyl)-α-D-N-acetylneuraminic acid (MU-NANA; Sigma, St. Louis, MO). Briefly, an aliquot of recombinant H5N1 neuraminidase (0.1 μg) was diluted in 90 μl of reaction buffer (50mM Tris-HCl, pH 7.2; 1 mM $CaCl_2$). The various dilutions of MU-NANA (10 μl) were added into designated reactions. The generation of fluorogenic 4-methylumbelliferyl in each reaction was detected in the real time at 460 nm with an excitation wavelength at 365 nm by a fluorescence plate reader (Fluoroskan Ascent from ThermoLabsystems, Finland). Enzyme kinetic parameters, km and kcat, were calculated by using Michaelis–Menten equation fitted with the KaleidaGraph computer program.

IC_{50} values, which are the concentrations of NA inhibitors that are required for inhibiting enzyme activity by 50%, were determined by assaying a standard amount of recombinant H5N1 neuraminidase in the presence of serial dilutions (from 10 to 150 μM) of inhibitors. After recombinant H5N1 neuraminidase (0.1 μg) was pre-incubated with serial dilutions of NA inhibitor in 90 μl of reaction buffer (50mM Tris-HCl, pH 7.2; 1 mM $CaCl_2$) for 30 minutes at RT, 10 μl of fluorogenic NA substrate MU-NANA was added at a final concentration, 100 μM, and the reaction mixture was then incubated for 1 h at 37°C. The release of fluorogenic 4-methylumbelliferyl in each reaction was measured at 460 nm with an excitation wavelength at 365 nm by a fluorescence reader (Fluoroskan Ascent). To obtain the IC_{50}, the does-response curves were fitted with the equation, $A(I) = A(0) \times \{1 - [I/(I+IC_{50})]$, where A(I) is the enzyme activity with inhibitor concentration I, A(0) is enzyme activity without inhibitor, and I is the inhibitor concentration.

Molecular docking and inhibitor search

The co-crystallized structure of NA and Oseltamivir (2HUO) was downloaded from Protein Data Bank (www.pdb.com). The active site was docked with the three inhibitors by using dock suite of Accelrys Discovery Studio 2.0 software (Accelrys, Inc.). All crystallographic water molecules, solvent molecules and ions were removed from the structure. Binding site was defined with the options of site opening = 5Å and grid resolution = 0.5 Å. Docking was performed with default values and "Dreidong" was selected

for Energy Grid Forcefield and "Minimizer" was selected for Minimization Algorithm. The highest ranked conformation was selected as the structural models.

Statistical Analysis

The experimental results were expressed as means ± S.E.

Results

Expression and characterization of recombinant H5N1 neuraminidase

The aim of the present study was the identification of new natural potential reversible non-peptidic inhibitors of NA (H5N1). The cDNA encoding N-terminal His-tagged ectodomain (63-449) of H5N1 neuraminidase protein was cloned into baculovirus genomic DNA. After the infection of Sf9 insect cells with recombinant baculovirus, His-tagged H5N1 neuraminidase protein was collected from culture media and purified by using Ni-NTA column. As shown in Figure 3, the purified H5N1 neuraminidase protein is observed on SDS-PAGE with molecular weight about 43 kDa and specifically recognized by H5N1 neuraminidase antibody.

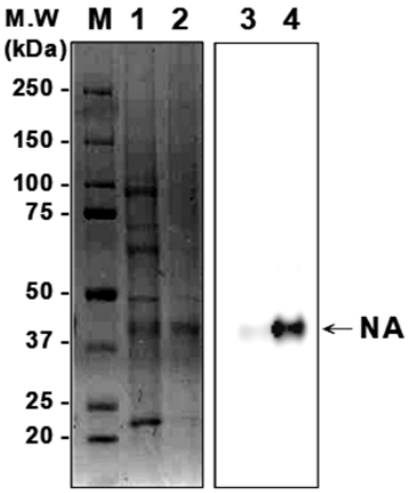

Figure 3: SDS-PAGE and Western Blot analysis of purified recombinant H5N1 neuraminidase. The aliquots (10 µg of each) of concentrated media (lanes 1 and 3) from recombinant baculovirus-infect insect cell culture and pooled elutes (lanes 2 and 4) from Ni-NTA column purification were loaded onto designated wells of SDS-PAGE.

To determine the enzyme kinetics of recombinant H5N1 neuraminidase, fluorogenic substrate 2'-(4-methylumbelliferyl)-α-D-N-acetylneuraminic acid (MU-NANA) of neuraminidase was employed to monitor the real-time activity of recombinant H_5N1 neuraminidase. The Km and kcat of the enzyme in using this fluorogenic substrate were measured to be 248 ± 11 µM and 2.5 min-1, respectively (Figure. 4).

IC50 measurements of the inhibitors

Recombinant NA protein and the fluorogenic substrate were used to screen for the NA inhibition of Kotomolide A, Linderanolide B and Isolinderanolide B (Figure 5). As summarized in Table 1, Kotomolide A, Linderanolide B and Isolinderanolide B inhibited recombinant NA from the H5N1 with the IC50 values is 38.6, 45.0 and 66.0 µM, respectively. As shown in Figure 4, these compounds share the same scaffold, a butanolide group, with different numbers of carbons in the alkyl groups. The alkyl groups provide hydrophobic interactions, but not critical for inhibition. Thus, the butanolide represents a novel carbon skeleton which binds to the active site of NA from H_5N1. The binding is mediated through charge-charge interaction and hydrogen bonding as shown by the computer modeling described below.

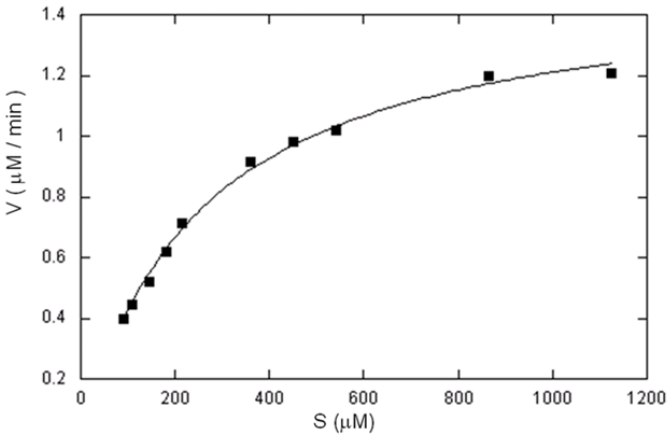

Figure 4: Substrate saturation curve for recombinant H5N1 neuraminidase. An aliquot of recombinant H5N1 neuraminidase was incubated with indicated concentrations of fluorogenic substrate MU-NANA at a real-time manner (0 to 10 min). The velocity (Y-axis) of the reaction was determined at various MU-NANA concentrations (X-axis). The values of km and kcat were measured to be 248 ± 11 µM and 2.5 min-1, respectively, by fitting the data with Michaelis-Menten equation using the KaleidaGraph computer program.

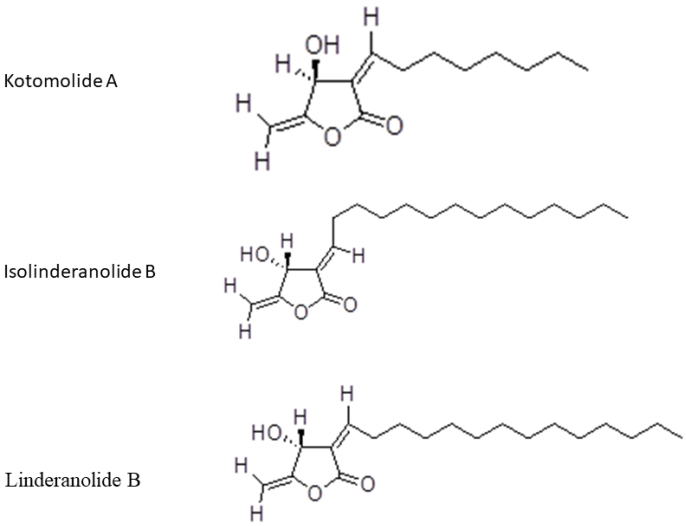

Figure 5: The chemical structure of Kotomolide A, Linderanolide B and Isolinderanolide B.

Table 1: The IC_{50} values of the natural product inhibitors against the NA.

Compounds	IC_{50} (μM)
Kotomolide A	38.6 ± 2.9 uM
Linderanolide B	45.0 ± 2.4 uM
Isolinderanolide B	66.0 ± 3.5 uM

Computer modeling to rationalize the inhibitor binding

We decided to explore the orientations of three compounds by virtual docking in the binding site of NA. On the basis of the literature data [13-17], we have derived a model of the NA active site (Figure 6A) to summarize the amino acids residues, which contribute to binding with the known inhibitors. The active site of NA has five well conserved binding sites, areas 1, 2, 3, 4, and 5. For computer modeling, NA structure composed of a tetramer of ~50 kDa glycosylated identical subunits with Oseltamivir bound was downloaded from PDB (2HUO). From X-ray structures, N-terminal hydrophobic sequence of NA is anchored on the lipid bi-layer, and a polypeptide fold of six β-sheets is arranged as the blades of a propeller. Each β-sheet is composed of four anti-parallel strands giving the topology of the letter 'W'. The active site lies on the propeller axis at the N-terminal ends of the first β-strand of each sheet [18]. Oseltamivir is bound with its hydroxyl group making hydrogen-bonds with the atoms of the side chains of Arg152 (area 4), Try347 and Arg371 (area 1).

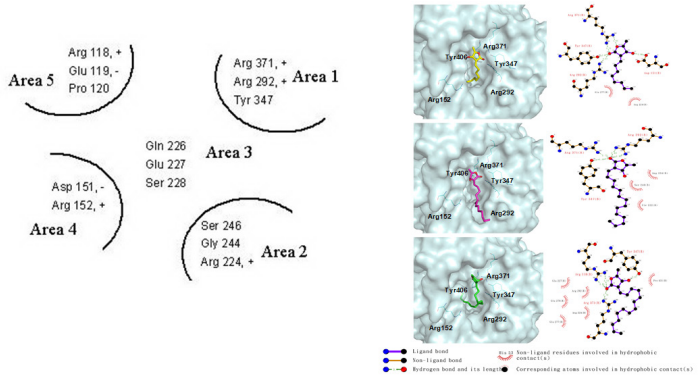

Figure 6: (A) Working model of the NA active site shown in a two-dimensional illustration. The distance of area 3 (center) is about 6 Å from area 1 and 5, and about 5 Å from area 2 and 4, while area 5 is about 6 Å from area 4 and 6 Å from area 3. The active site is a cavity about 500 Å3. (B) Computer docking of inhibitors in the active site of NA. Interactions of Kotomolide A (yellow), Linderanolide B (purple) and Isolinderanolide B (green) with wild type NA. The complex structure of NA (2HUO) was obtained from PDB data bank. The complexed structures were calculated from DS modeling. Oxygen atoms are colored in red. The figure was prepared using the PyMol and LigPlot programs.

Kotomolide A, linderanolide B and isolinderanolide B were docked into the active site as shown in Figure 6B. As compared with the binding mode of the NA with Oseltamivir, Kotomolide A has interactions with the side chains of Asp151, Arg224, Glu277, Arg292, Try347, and Arg371 (Ligplot is shown in the right panel). Butanolide group makes 5 hydrogen bonds with Asp151 (area 4), Arg292, Try347, and Arg371 (area 1), whereas the alkyl group forms hydrophobic interactions with the main chains of Arg224 and Glu277 in areas 2 and 3. Linderanolide B forms 4 hydrogen-bonds with Arg292, Try347, and Arg371 (area 1), so does the Isolinderanolide B to the Arg118 (area 5), Try347, and Arg371 (area 1). The alkyl side chains of these three compounds all have similar hydrophobic interactions with the corresponding atoms (area 2, 3).

Discussion

Chinese medicines are important resources for medicine and healthy food to get better life for thousands of years. Now in the developed countries of Europe and America, natural herbal medicines are generally accepted. In 2002, the WHO announced an important draft called the Global Traditional Medicine Strategy, which indicated that the enormous potential for natural products needs to be further investigated. Furthermore, more than 60 % of commercial medicines derived from natural products and their analogues. In recent years, scientists work on how natural small molecules modulate the function of genes, proteins, enzymes, and receptors in different human diseases. Kotomolide A was firstly isolated from the leaves of Cinnamomum kotoense [10]. Studies have shown that kotomolide A induces apoptosis in human breast cancer cells and lung cancer cells by inferring with cell cycle progression [19,20]. The other two purified butanolide compounds, isolinderanolide B and linderanolide B from C. subavenium, were evaluated for the cytotoxic effects in the human bladder cancer cells and melanoma cells [21,22]. Isolinderanolide B induces apoptosis and blocks cell cycle progression in bladder cancer cells [21]. Linderanolide B has tyrosinase inhibition activity and displays synergic effect in B16F10 cells [22].

NA is thought to enhance influenza viral mobility via hydrolysis of the α-(2, 3)- or α-(2,6)-glycosidic linkage between a terminal sialic acid (Neu5Ac) residue and its adjacent carbohydrate moiety on the host receptor [23]. This cleavage allows progeny virus particles budding from infected cell surfaces to be released [24,25]. The discovery of inhibitors of NA for the treatment of influenza infection has been an active area of research [26,27]. Some known drugs including zanamivir and oseltamivir have been developed for treatment of severe influenza diseases. However, due to the hypermutational property of H5N1 avian flu viruses, drug-resistant strain has occurred. Side effect was also reported for the drug. A new drug commonly used to prevent the disease without side effect is desired. Such a drug may be derived from natural products. In the new findings presented here, these natural compounds displayed promising potency in the enzyme-based NA assays and may be developed as therapeutic or preventive agents for both human and bird flu. We will further optimize lead compounds by medicinal chemistry to obtain more potent inhibitors.

Kotomolide A, isolinderanolide B and linderanolide B have the same scaffolds to inhibit NA. To locate their binding site on NA, DS modeling was performed. Previous NA inhibitors as substrate mimics utilized amines and hydroxyl groups to bind the negatively charged amino acid residues, Glu119, Glu227, and Asp151 [17,28,29]. The availability of crystal structures of inhibitor–NA complexes have enabled a detailed analysis of the structural basis

for potent inhibition [30]. The butanolide derivatives bind to the active site with several interactions perhaps including the hydrogen bonds with the side chains of Arg118, Asp151, Arg292, Try347, and Arg371. Docking studies on the crystallized structure of NA will led us to the understanding of the inhibitory mechanisms on butanolide analogues. The information obtained from computer modeling approach is useful for deriving more potent inhibitors [31,32].

Conclusions

In the present study, we investigated kotomolide A, isolinderanolide B and linderanolide B have anti-viral activities. These results revealed evidence that these compounds possessed neuraminidase inhibition and decrease viral replication. Therefore, we considered that kotomolide A, isolinderanolide B and linderanolide B possess great potential to become agents for preventing virus infection in the future.

Acknowledgments

This investigation was supported by a grant from the National Taiwan University awarded to S. L. Liu and the Yuan's General Hospital (YGH-22-006) awarded to C. T. Chang.

References

1. Stevens J, Blixt O, Tumpey TM, et al. Structure and receptor specificity of the hemagglutinin from an H5N1 influenza virus. Science. 2006; 312: 404-410.
2. Scholtissek C, Rohde W, Von Hoyningen, V, et al. On the origin of the human influenza virus subtypes H2N2 and H3N2. Virology. 1978; 87: 13-20.
3. Saito A. Physiopathology and therapy in patients with respiratory tract infections. Nippon Naika Gakkai Zasshi. 1993; 82: 433-436.
4. Johnson NP, Mueller J. Updating the accounts: global mortality of the 1918-1920 "Spanish" influenza pandemic. Bull Hist Med. 2002; 76: 105-115.
5. Taubenberger JK, Reid AH, Lourens RM, et al. Characterization of the 1918 influenza virus polymerase genes. Nature. 2005; 437: 889-893.
6. Tumpey TM, Basler CF, Aguilar PV, et al. Characterization of the reconstructed 1918 Spanish influenza pandemic virus. Science. 2005; 310: 77-80.
7. Le QM, Kiso M, Someya K, et al. Avian flu: isolation of drug-resistant H5N1 virus. Nature. 2005; 437: 1108.
8. Liao JC. Lauraceae in Flora of Taiwan, 2nd ed. Editorial Committee of the Flora of Taiwan: Taipei 1996; 2: 443-483.
9. Chen FC, Peng CF, Tsai IL, et al. Antitubercular constituents from the stem wood of Cinnamomum kotoense. J Nat Prod. 2005; 68: 1318-1323.
10. Chen CH, Lo WL, Liu YC, et al. Chemical and cytotoxic constituents from the leaves of Cinnamomum kotoense. J Nat Prod. 2006; 69: 927-933.
11. Chen CY. Butanolides from the Stems of Cinnamomum kotoense. Nat Prod Commun. 2006; 1: 453-455.
12. Chen CY, Chen CH, Wong CH, et al. Cytotoxic constituents of the stems of Cinnamomum subavenium. J Nat Prod. 2007; 70: 103-106.
13. Taylor NR, von Itzstein M. Molecular modeling studies on ligand binding to sialidase from influenza virus and the mechanism of catalysis. J Med Chem. 1994; 37: 616-624.
14. Varghese JN, Epa VC, Colman PM. Three-dimensional structure of the complex of 4-guanidino-Neu5Ac2en and influenza virus neuraminidase. Protein Sci. 1995; 4: 1081-1087.
15. Crennell SJ, Garman EF, Philippon C, et al. The structures of Salmonella typhimurium LT2 neuraminidase and its complexes with three inhibitors at high resolution. J Mol Biol. 1996; 259: 264-280.
16. von Itzstein M, Dyason JC, Oliver SW, et al. A study of the active site of influenza virus sialidase: an approach to the rational design of novel anti-influenza drugs. J Med Chem. 1996; 39: 388-391.
17. von Itzstein M, Wu WY, Kok GB, et al. Rational design of potent sialidase-based inhibitors of influenza virus replication. Nature. 1993; 363: 418-423.
18. Nicholson KG, Wood JM, Zambon M, et al. Lancet. 2003; 362: 1733-1745.
19. Chen CY, Hsu YL, Tsai YC, et al. Kotomolide A arrests cell cycle progression and induces apoptosis through the induction of ATM/p53 and the initiation of mitochondrial system in human non-small cell lung cancer A549 cells. Food Chem Toxicol. 2008; 46: 2476-2484.
20. Kuo PL, Chen CY, Tzeng TF, et al. Involvement of reactive oxygen species/c-Jun NH(2)-terminal kinase pathway in kotomolide A induces apoptosis in human breast cancer cells. Toxicol Appl Pharmacol. 2008; 229: 215-226.
21. Shen KH, Lin ES, Kuo PL, et al. Isolinderanolide B, a butanolide extracted from the stems of Cinnamomum subavenium, inhibits proliferation of T24 human bladder cancer cells by blocking cell cycle progression and inducing apoptosis. Integr Cancer Ther. 2011; 10: 350-358.
22. Hseu YC, Cheng KC, Lin YC, et al. Synergistic Effects of Linderanolide B Combined with Arbutin, PTU or Kojic Acid on Tyrosinase Inhibition. Curr Pharm Biotechnol. 2015; 16: 1120-1126.
23. Ward CW. Structure of the influenza virus hemagglutinin. Curr Top Microbiol Immunol. 1981; 94-95: 1-74.
24. Palese P, Tobita K, Ueda M, et al. Characterization of temperature sensitive influenza virus mutants defective in neuraminidase. Virology. 1974; 61: 397-410.
25. Murti KG, Webster RG. Distribution of hemagglutinin and neuraminidase on influenza virions as revealed by immunoelectron microscopy. Virology. 1986; 149: 36-43.
26. Chand P, Babu YS, Bantia S, et al. Design and synthesis of benzoic acid derivatives as influenza neuraminidase inhibitors using structure-based drug design. J Med Chem. 1997; 40: 4030-4052.

27. Wang GT, Wang S, Gentles R, et al. Design, synthesis, and structural analysis of inhibitors of influenza neuraminidase containing a 2,3-disubstituted tetrahydrofuran-5-carboxylic acid core. Bioorg Med Chem Lett. 2005; 15: 125-128.
28. Colman PM. Zanamivir: an influenza virus neuraminidase inhibitor. Expert Rev Anti Infect Ther. 2005; 3: 191-199.
29. Varghese JN. Development of neuraminidase inhibitors as anti-influenza virus drugs. Drug Develop Res. 1999; 46: 176-196.
30. Varghese JN, Colman PM. Three-dimensional structure of the neuraminidase of influenza virus A/Tokyo/3/67 at 2.2 A resolution. J Mol Biol. 1991; 221: 473-486.
31. Blundell TL, Structure-based drug design. Nature. 1996; 384: 23-26.
32. Hardy LW, Malikayil A. The impact of structure-guided drug design on clinical agents. Curr Drug Discov. 2003; 3: 15-20.